DOI: https://doi.org/10.24425/amm.2025.156239

M.A. GONZÁLEZ GARCÍA<sup>©1</sup>, A. DOBKOWSKA<sup>©1</sup>, W. ŚWIĘSZKOWSKI<sup>©1\*</sup>

### Zn AND Zn ALLOYS FOR CARDIOVASCULAR STENTS: INFLUENCE OF MANUFACTURE TECHNIQUES ON MICROSTRUCTURE, MECHANICAL AND CORROSION PERFORMANCE

This review aims to explore the processing-structure-property relationship of Zn and Zn-based alloys developed for biodegradable cardiovascular stents. It assesses how conventional and advanced manufacturing techniques, including casting, extrusion, laser cutting, and additive manufacturing, affect the microstructure, mechanical performance, and degradation behavior of Zn-based materials. Particular emphasis is placed on the potential of additive manufacturing due to its ability to enhance microstructure, corrosion, and mechanical properties by adjusting the processing parameters and producing patient-specific stent geometries with enhanced precision and functionality. The review also addresses the unique processing challenges associated with Zn, such as high vaporization during laser processing. Additionally, the review identifies key knowledge gaps and outlines directions to support future research to advance Zn-based stents toward clinical translation as biodegradable cardiovascular stents.

Keywords: Biomaterials; zinc; additive manufacturing; cardiovascular stents; manufacturing techniques

#### 1. Introduction

#### 1.1. Cardiovascular diseases and treatments

Cardiovascular diseases (CVD), such as coronary artery disease (CAD), have been found to increase the risk of death in both developed and developing countries [1]. In 1996, 29% of the world's mortality rate was attributed to cardiovascular diseases; almost half of these deaths were estimated to be caused by CAD. By 2020, CAD was expected to be the most significant cause of worldwide disease burden [2]. Recent findings provided by Chong et al. [3] indicate that cardiovascular diseases, especially atherosclerotic diseases related to CAD, are estimated to rise within the next few decades due to risk factors such as high blood pressure, dietary risks, and high cholesterol that could maintain CVD prevalence constant between 2025 to 2050. Supporting this, the Global Cardiovascular Risk Consortium in 2025 [4] reports that risk factors as blood pressure, diabetes, smoking, non-HDL cholesterol levels, and body mass index account for around 50% of the total global burden of cardiovascular disease. CAD consists of the narrowing of the artery due to plaque deposits beneath the endothelium. The deposits are mainly composed of cells, fats, cholesterol, calcium, cellular debris, and fibrin that can lead to a diminished blood vessel artery lumen, restrict blood flow, and inadequate nutrients and oxygen supply to the heart [5], known as atherosclerosis [6]. It causes stable or unstable angina, myocardial infarction, transient cerebral ischemic attacks, stroke, or sudden cardiac death [1].

The most common methods for atherosclerosis treatment (as shown in Fig. 1) are i) medications, ii) coronary artery bypass grafting (CABG), and iii) the utilization of cardiovascular stents. Those methods are well-known and have been used for a long time. However, their application is limited due to several side effects [7]. Medications can lead to adverse effects such as intolerance to drug administration or, in worse cases, an insufficient response to avoid further plaque formation [8]. For example, aspirin therapy may cause bleeding and allergic reactions [9], while statin therapy may produce myalgias, diarrhea, and arthralgia [10]. CABG consists of a very invasive surgery in which an alternative artery or vein from the body is used to bypass the blocked part [6]. It was successfully implemented in 1961 [11]. Nevertheless, it is commonly used in severe cases of coronary artery blockage [12] since it can lead to complications during the perioperative stage [13]. Stents are the most common solution for less complex cases, mainly from polymers and metals [7]. These are tubular implants that give the stenotic arteries or other

<sup>\*</sup> Corresponding author: wojciech.swieszkowski@pw.edu.pl



WARSAW UNIVERSITY OF TECHNOLOGY, FACULTY OF MATERIALS SCIENCE AND ENGINEERING, BIOMATERIALS GROUP, MATERIALS DESIGN DIVISION, 141 WOLOSKA STR., 02-507, WARSAW, POLAND

non-vascular conduits mechanical strength until the risk of full closure disappears; these can work as self-expanding or balloon-expandable stents, also called angioplasty procedure, the latter the most common form for cardiovascular stents application [14].

#### 2. Materials used for cardiovascular stents

Cardiovascular stents have been used since 1977 [15], and they can be classified primarily into two categories: permanent (non-resorbable) and temporal (bioresorbable) [16]. Among permanent implants, 316L, CoCr, pure Ti, and its alloys (e.g., Ti-6Al-4V and NiTi) are primarily used [17]. Bioresorbable stents are produced from two types of materials: i) polymers from lactic acid, glycolic, and caprolactone families [18], and ii) metals such as Fe [19], Mg [20], and Zn [21]. Polylactide is one of the most common biodegradable polymers used; nevertheless, it has limitations due to its poor toughness, low mechanical strength, slow degradation rate, hydrophobicity, and difficulty modifying its surface. Alternatively, polymer-based materials are used as coating material, with the possibility of incorporating drugs [22]. Over the last decade, bioresorbable metal stents have become an attractive treatment for interventional cardiology. Unlike polymer-based and permanent metallic stents, bioresorbable metals are known to be essential for the human body through cellular functions as well as overcome and provide enhanced strength and radiopacity, which are shortcomings of polymerbased stents [23]. Also, grave consequences that mainly occur in permanent stents can be prevented. The most severe complications are in-stent recurrence of stenosis (in-stent restenosis), arterial damage [5], chronic inflammatory response [24], late stent thrombosis, and stent fractures [25]. All of these can cause serious life-threatening complications, which might be avoided by using bioresorbable metallic stents.

Among metallic biodegradable metals, only three groups have been used: Fe, Mg, Zn, and their alloys. When compared to Mg, Fe exhibits superior mechanical properties. However, it shows a slow degradation rate that results in long-term retention of its corrosion products within the artery. Conversely, Mg tends to corrode too rapidly, which decreases its mechanical integrity during the stent application [26]. Zn-based materials avoid several major drawbacks observed in Fe- and Mg-based materials, such as long-term retention of corrosion products or intense hydrogen gas release (both cause damage to surrounding tissues, leading to inflammation or even pain). In terms of standard electrode potential, Zn has an intermediate value (-0.76 V vs SHE) between Fe (-0.44 V vs SHE) and Mg (-2.37 V vs SHE) [17]. Its degradation rate matches the healing period of the endothelium [23], and it has good biological properties as it exerts cardioprotective roles against atherosclerosis and sufficient mechanical properties required for bioresorbable applications in the biomedical field [27]. Among the metallic bioresorbable stents, only Mg has achieved clinical trials. The Biotronik company produced a bioresorbable coronary artery stent called Magmaris (previously known as DREAMS 2G) [28] made from WE43 (Mg-RE-Zr series). This stent is available in

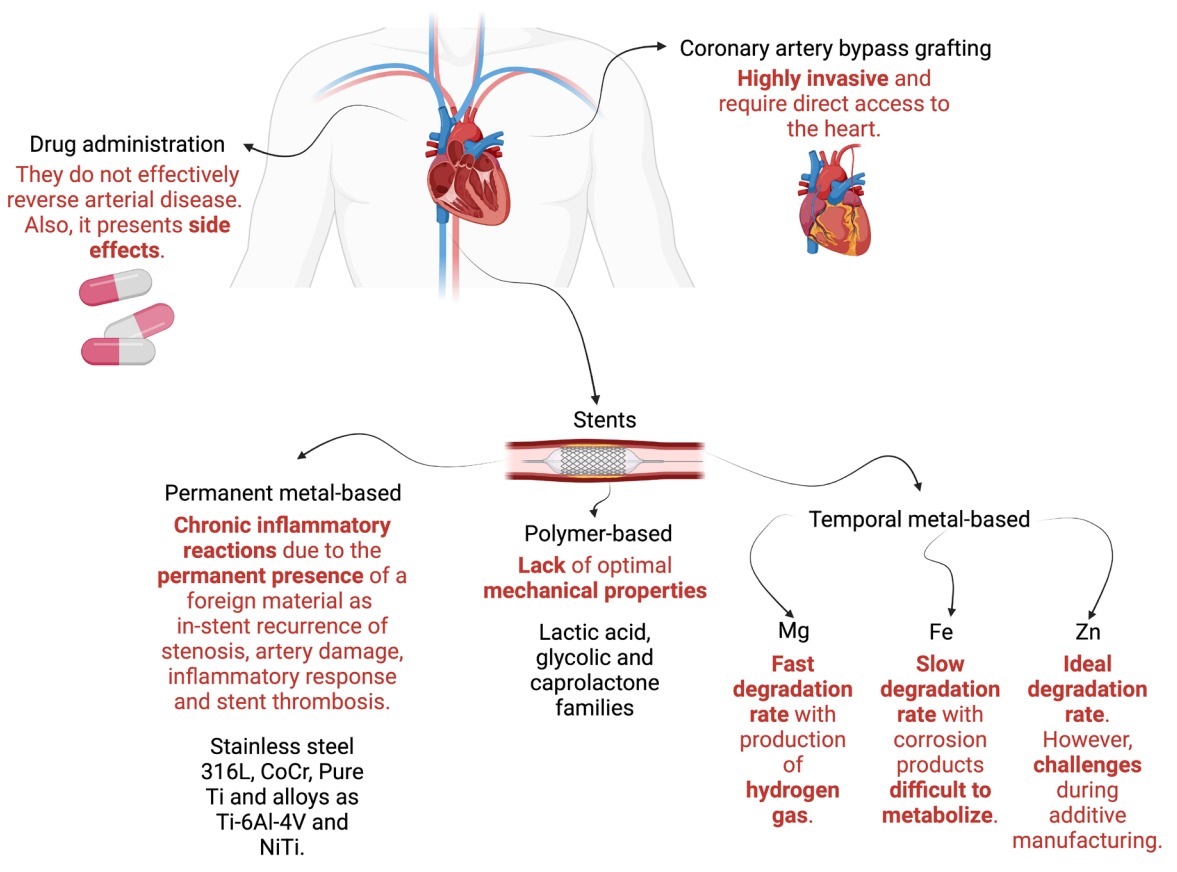


Fig. 1. Schematic graph for CAD available treatments with a focus on stents. Created in BioRender

two diameter sizes: 3 and 3.5 mm, and 15, 20, or 25 mm in length. Magmaris has been investigated under clinical trials and achieved almost 80% success due to vasomotion function recovery after 6 months [29], and it is still under clinical observation through several investigations. To extend the number of clinical applications and overcome obstacles related to Mg quick degradation, attention has been lately focused on Zn and its alloys.

#### 2.1. Zn properties

Zn is considered a micronutrient in the human body which daily intake is about 6.5 mg to 15 mg [17] and in a lower quantity it can lead to a deficiency producing a greater risk of infection, loss of cognitive function, memory, and even behavioral problems [30]. Zn plays an essential role in the human body's biochemical functions and is required by nearly 300 enzymes, being a catalytic, co-catalytic, and structural part for the proper folding of proteins [31]. Zn also participates in cell division, cell growth, and wound healing [32], and it is crucial in the immune system. Rink et al. [33] reported that Zn synchronizes the immune function, and both increasing and decreasing Zn levels result in an immune function disturbance.

It is essential to mention that the main product of Zn degradation, Zn<sup>2+</sup>, is considered fundamental for cellular processes and for inducing slightly antimicrobial activity that can slow down biofilm formation [27]. This is crucial because infections are associated with a diverse range of implant surgeries with both clinical and economic consequences. In the case of patients with cardiovascular implants, a higher mortality and severe disabilities are attributable to infections (most commonly caused by *Staphylococcus aureus and Staphylococcus epidermidis* [34]), with a rate of infection of about 2%. However, the complication may be lethal in almost 90% of cases [35].

Zn started to be investigated as a degradable biomaterial by Wang et al. [36] in 2007. The authors studied the corrosion behavior of casted Zn-Mg (35, 40, and 45 wt.%) in SBF solution, and they proved that regardless of the Zn alloy composition, there is a tendency in the passivation film to form and compact (up to 90 h immersion) and break (especially after 160 h). The broken passive layer led to an increase in pH values due to Zn<sup>2+</sup> and Mg<sup>2+</sup> release. In 2013, Bowen et al. [21] examined Zn as a bioabsorbable cardiac stent material during in vivo tests in the murine aorta of male Sprague-Dawley rats. During 1.5 and 3 months in vivo, the Zn wires showed uniform corrosion, which changed to localized one after 4.5 and 6 months, with the surrounding tissues adhering to areas of corrosion damage. In addition, they found that the penetration rate significantly increased from ~10 μm/year after 1.5 months to ~40 μm/year after 4.5 months of implantation. Such a period of slow degradation during the first 3 months sufficiently assured mechanical integrity; afterward, quick disintegration occurred. It was also reported that Zn wires exhibited antiatherogenic properties, a desirable degradation compared to Fe and its alloys, and harmless degradation compared to Mg and its alloys. In 2019, the US company PediaStent developed a Zn-based bioresorbable stent called ZeBRA [37]. ZeBRA, which is still under development, has been designed for congenital heart defects in pediatric applications [38]. *In vivo* studies indicate that ZeBRA fulfilled the desired criteria for stents, such as radial strength, ultralow profile, radiopacity, and low thrombogenicity [37]. It also has anti-inflammatory properties that attenuate neointimal proliferation and in-stent stenosis [39].

Due to its biocompatibility, biodegradability, and possible antibacterial properties, Zn and its alloys are being investigated for biomedical purposes, including cardiovascular stenting applications. While several reviews address Zn-based biodegradable materials for cardiovascular applications in their general behavior, these often focus principally on individual aspects as biological performance, corrosion behavior, or alloying strategies. For instance, Rao et al. [40] examined biodegradable Zn alloys with emphasis on clinical applications. Zhou et al. [41] study the additive manufacturing of Zn for biomedical applications, while Shi et al. [42] emphasize the design of biodegradable Zn alloys through second phases. Liu et al. [43] provided a general progress on both Mg and Zn alloys for biodegradable vascular stent applications. Additionally, Limón et al. [44] provided a review on laser powder bed fusion for Fe and Zn alloys for medical implants. In contrast, the presented review aims to provide a comprehensive examination of the current state-of-the-art in Zn and Zn alloys research for cardiovascular stenting applications. Particular emphasis is placed on the advancements in manufacturing techniques, ranging from casting to new emerging approaches such as additive manufacturing, and their influence on the microstructure, mechanical, and corrosive properties for both in vitro and in vivo tests. The objective is to identify processingproperty relationships that may be useful as a guide for the future development of metallic biodegradable cardiovascular stents.

# 3. Manufacturing requirements for biodegradable cardiovascular stents

Stent production is challenging due to critical requirements to ensure the safety and efficacy of the stents as a treatment for CAD. Since there are no requirements for biodegradable stents that have been standardized, many authors have made guidelines on which properties should be fulfilled by biomaterials used for bioabsorbable cardiovascular stents. The following recommendations and insights have emerged.

# 3.1. Material criteria for biodegradable cardiovascular stents

In general, the size of metallic stents is about 2-4 mm in diameter and 15-20 mm in length [45]. For balloon-expandable stents, materials should have sufficient formability to be susceptible to plastic deformation and remain in their expanded shape except for a slight recoil [46]. Radial strength and compression

pressure are strongly indispensable properties for a stent. The weak radial strength may provoke residual stenosis and separate the stent struts from the arterial wall. No specific parameter describes this property; however, based on *in vitro* tests, 30 kPa is considered a minimum requirement for compression resistance [46]. Simultaneously, stents should show a low yield stress to allow balloon expansion deployment, a high elastic modulus that permits a minimal recoil, and a high strength that can be achieved through expansion (work hardening) to maintain mechanical support during the vascular wall repair before it erodes gradually [47]. The expected time for an atherosclerotic artery to heal may be about 3 to 6 months [48]. Bowen et al. [7] explained that there are several criteria and constraints to take into account for bioabsorbable stents, among them:

- complete stent absorption should occur between 12 and 24 months of implantation in the human body but maintain mechanical integrity for at least 3-6 months,
- ii) mechanical properties: yield strength should be higher than 200 MPa; the ultimate tensile strength larger than 300 MPa; the yield strength in its elastic modulus ratio major than 0.16; the elongation to failure higher than ~15%, the elastic recoil on expansion lower than 4% and its resistance to cyclic fatigue over 10-20 million cycles,
- iii) homogenous microstructure with a grain size smaller than  $30 \mu m$ ,
- iv) corrosion rate should be about 0.02 mm/year or less.

# 3.2. Surface characteristics and their role in stent performance, with emphasis on Zn-based modifications

Surface characteristics are essential to reduce restenosis, accelerate endothelialization, and enhance local healing. Surface properties are focused on three major areas: i) improvement of the blood contact, ii) enhancement of the endothelial cell migration, attachment, and proliferation, and iii) also working as a drug release in porous surface layers [49]. Wang et al. [50] investigated the stent design as a component that can induce changes in blood flow. It was concluded that the stent strut protrusion provoked a stagnation zone as the stent implantation produced an uneven pressure gradient distribution [50]. Briguori et al. [51] studied the impact of strut size in a <3 mm vessel, and it was reported that thin struts (<0.10 mm) may reduce the restenosis rate by up to 56% for angiographic restenosis. With the same purpose, Chen et al. [52] studied a new method to minimize flow disturbance by producing streamlined cross-sectional wires. Gundert et al. [53] analyzed the stent design and found that ~40° for the intrastrut angle was optimal for the stent hemodynamics. Pant et al. [54] found that the length of connectors in the cross-flow directions and the alignment with the flow strongly relate to the hemodynamics disturbance. Jing et al. [55] discovered that endothelial cells spread better on the nanopatterned surfaces, allowing cells to align along nano-lines that simulate natural vessel walls compared to random nanostructures.

Physical or chemical surface modification strategies may also be helpful in coating production to improve physiological response. These coatings are classified into inorganic, polymer, or composite. Inorganic materials include oxides, hydroxides, phosphates, ceramics, and metal coatings [56]. For example, Su et al. [57] studied Zn phosphate, Zn oxide, and Zn hydroxide and found that Zn phosphate, in particular, improves cell viability and hemocompatibility. Alternatively, polymer coatings can be favorable as drug release systems. For example, permanent polymer (PBMA, PEVA, PVDF, among others), polymer-free (micropores, grooves, or texture surface), or biodegradable coatings (PLLA, PLG, Mg, hydroxide, chitosan, among others) with various drugs that may support as immunosuppressive, anti-proliferative, antithrombotic, or anti-inflammatory [58], such as Everolimus, Myolimus, Novolimus, and Paclitaxel; however, Sirolimus is mainly used [59] due to its antifungal and immunosuppressive properties [60]. Also, it is associated with minimal neointimal hyperplasia when employed as a coating for metallic stents [61]. Among other types of coatings that have been employed for Zn-based materials are composite systems, which consist of inorganic-inorganic, inorganic-polymer, and polymerpolymer combinations. These hybrid types of coatings are designed to obtain the advantages of multiple material types [56].

The final sterilization is a method that can influence stent surface properties. Seitz et al. [62] proved that the mechanical properties are susceptible to various sterilization methods; however, they depend on the alloy and sterilization process. Li et al. [63] provided important insights into the influence of sterilization treatments and how they affect Zn's surface characteristics, biodegradability, and cytocompatibility. The authors tested Zn and Zn-3Cu (wt.%) under gamma irradiation, hydrogen peroxide gas plasma, and steam autoclave. It was reported that steam autoclave sterilization produced the most remarkable changes in the degradation, corrosion behavior, and cytocompatibility due to the formation of an inhomogeneous ZnO layer; meanwhile, gamma irradiation and hydrogen peroxide gas plasma sterilizations did not have any apparent adverse effects or alterations on the material surface.

### 4. Manufacturing techniques for Zn-based biodegradable cardiovascular stents

Choosing the most appropriate manufacturing method is the principal and crucial step to obtaining stents' desired shape and size with optimized degradation rates, biocompatibility, and mechanical properties. There are a variety of processes currently used for Zn and its alloys, which can be divided into two categories: conventional methods (casting, plastic deformation such as drawing or extrusion) and advanced processing techniques (powder metallurgy, severe plastic deformation, additive manufacturing or electroforming) [30]. The second group is beneficial for enhancing Zn properties. Cast Zn is soft and brittle, but its properties are improved through alloying and plastic deformation [64]. Brittleness can be eliminated, and the yield strength

can increase to 200 MPa, making it suitable for clinical devices. Among the second group of manufacturing techniques, the most common methods used for cardiovascular stenting production are laser cutting, electrospinning, and additive manufacturing [65]. Nevertheless, Zn stent trials and prototypes have been chiefly manufactured following the production chain of casting, extrusion or rolling, tube drawing, and laser cutting with or without post-production processes.

Current review shows that various manufacturing methods have been used so far to produce materials for biodegradable stent applications. The most common of them are listed in Fig. 2.

It is essential to mention that various studies dedicated to understanding the behavior of Zn as cardiovascular stents are being investigated without completing the final shape of stents. Casting, extrusion, rolling, or drawing is enough to produce wires and tubes, which are being studied with a special focus on further application as stents. Additive manufacturing has gained attractiveness due to its feasibility of personalized implants according to patient requirements and reducing manufacturing steps.

### 4.1. Commercially purchased and laboratory extruded Zn wires

In 2017, Drelich et al. [66] implanted commercially purchased Zn wires (Goodfellow with a 99 + % purity in a size of 0.25 mm diameter) into the abdominal aorta of rats for up to 20 months. A linear area reduction and penetration rate of up to 60% cross-sectional area reduction were discovered, indicating

that the strut size may produce slower degradation. These results suggest that it cannot meet the guidelines stating that the implant's complete absorption should occur around 12-24 months [7]. Zhao et al. [67] studied Zn-0.1Li (wt.%) alloys processed by hot extrusion using a 10 MN extruder (SMS MEER GmbH), followed by wire drawing at 180°C through multiple passes to reduce the diameter to 0.25 mm. The resulting wires exhibited an ultimate tensile strength of about  $274 \pm 61$  MPa and  $17 \pm 7\%$  ductility. The corrosion rate after implantation for 2 and 12 months in the abdominal aorta of Sprague-Dawley rats was calculated to be 0.008 mm/year and 0.045 mm/year, correspondingly. Jin et al. [68] fabricated extruded Zn-Mg wires with an initial diameter of 13 mm using hot extrusion at 150°C, followed by wire drawing to a final diameter of 0.25 mm. The alloys contained varying Mg contents: 0.002, 0.005, and 0.08 (wt.%). Subsequently, mechanical properties and arterial biodegradation during in vivo were evaluated through implantation in Sprague-Dawley rats. The best mechanical properties were found to be for Zn-0.08Mg with an elongation of about 40%, yield strength of about 221 MPa, and tensile strength of about 339 MPa. However, with the increasing Mg content, the biocompatibility was lowered due to the formation of Mg<sub>2</sub>Zn<sub>11</sub>, which may cause harmful macrophage responses. Guillory et al. [69] investigated high-purity (99.99%) Zn wires (0.25 mm) purchased from Sigma-Aldrich, which were modified using two different processes to produce oxide films: electropolishing and anodizing. The effects of these treatments were evaluated through both in vitro and in vivo studies. Results indicated that the corrosion behavior after electropolishing produced a porous and nonuniform film with non-regular thickness

# Manufacturing techniques used for Zn cardiovascular stents Conventional and advanced manufacturing techniques

Casting

Extrusion

\*Wire drawing Tube drawing

\*Wires are also commercially available

Laser cutting

Photo-chemical etching

Post-processing treatments

Electrochemical polishing

Anodizing

Chemical etching

Physical vapor deposition
(PVD)

Spray coating

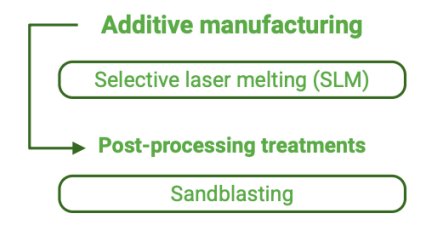


Fig. 2. Schematic showing the current methods used for Zn cardiovascular stent manufacturing found in the literature. Created in BioRender

(from 2  $\mu$ m to 10  $\mu$ m) with localized corrosion. In contrast, the anodizing method allowed densification of the coating that protected the sample for 28 days of immersion, showing improved biocompatibility. However, it was concluded that anodized samples may not be appropriate for stenting applications due to the high risk of cracking during balloon expansion.

#### 4.2. Tube drawing

Another method used tube drawing. The developed process chain for micro-tubes produced from Zn and its alloys consists of drilling and extruded billet followed by several cold-rolling operations and multi-pass drawing [70]. In 2015, Liu et al. [71] produced mini-tubes using ultra-pure Zn finished via electrochemical polishing. The in vitro and cytotoxicity tests in Hank's balanced salt solution (HBSS) using human umbilical vein endothelial (ECV304) and vascular smooth muscle (VSMC) cells showed optimal results for both ECV304 (87.38  $\pm$ 0.73% and  $84.48 \pm 1.68\%$ ) and VSMC (79.30  $\pm 5.94\%$  and  $82.98 \pm 4.32\%$ ) cell cultures. The tensile strength and elongation achieved  $44.50 \pm 1.76$  MPa and  $7.57 \pm 0.20\%$ , respectively, which were higher when compared to plate-shaped samples  $(35.31 \pm 2.21 \text{ MPa} \text{ and } 9.37 \pm 1.24\%)$ . The corrosion rate of Zn mini tubes was lower than that of pure Mg, about 0.027 to 0.036 mm/year. In 2016, Wang et al. [72] produced mini tubes from Zn-5Mg-1Fe (wt.%) with strength and ductility of about 220 MPa and 20%, respectively, and a corrosion rate analyzed in SBF of 0.062 mm/year. Afterward, they produced stents using laser etching and electrochemical polishing and found that these did not show breaking or cracking before and after being expanded. In 2019, Dai et al. [73] studied pure Zn and Zn with 0.5Li wt.% addition, and they showed that mini tubes had an ultimate tensile strength of 296.2 MPa and elongation of about 33%. The principal strengthening mechanism in Zn-Li alloy was related to the pinning effect around the nano LiZn<sub>4</sub> precipitates. In 2022, the Zn-0.1.Mg-1Mn (wt.%) was used to extrude tubes with an outer diameter of 12 and 2 mm thickness [74]. The authors analyzed the impact of extrusion temperature (100, 200, and 300°C) on the mechanical properties. The microstructural changes obtained during extrusion were the most suitable for producing material with a high ultimate strength of 405 MPa and yield strength of 380 MPa. The elongation of those tubes was around 14%. The other chemical composition of Zn alloys with a unique application for vascular application was studied by Lou et al. [75] in 2024. They fabricated tubes with the final dimensions of 3.5 mm diameter and 0.2 mm length from Zn-0.5Mn-0.05Mg (wt.%). The results obtained for yield tensile strength  $(277 \pm 2.9 \text{ MPa})$ , ultimate tensile strength  $(330 \pm 3.3 \text{ MPa})$ , and elongation (39.8  $\pm$  5.25%) satisfy the biodegradable requirements. They proved that the increase of pass rolled increases the strength due to a more uniform microstructure, texture evolution, and grain size refinement.

Zn alloys studied during the last decade by Liu et al. [71], Wang et al. [72], Dai et al. [73], Ren et al. [74], and Lou et al. [75] shown promising mechanical properties to be potentially used for vascular applications. However, their degradation and biological properties must be analyzed further.

#### 4.3. Laser cutting

Laser cutting is the principal manufacturing technique for producing exact and specific shapes of stents [5]. It is a thermalbased, non-contact process to cut complex shapes with high precision and accuracy [76]. It consists of a high-energy-density laser beam focused on a workpiece surface; the thermal energy is absorbed, which heats and transforms the workpiece volume into a molten, vaporized, or chemically changed state that the flow of high-pressure assist gas jet can easily remove [77]. The first reports on pure Zn stents produced by laser cutting with surface finalized via electrochemical polishing were published by Yang et al. [78] in 2017. They produced stents with the size of 3 mm in diameter and 10 mm in length, and the strut thickness was 165 µm. The stents were implanted in the abdominal aortas of Japanese rabbits using angiography for 3 days, 1, 3, 6, and 12 months. The stents maintained mechanical integrity for at least 6 months, and after 12 months, the stent degraded by about 42%. The degradation products showed biocompatibility with no severe inflammation and no apparition of platelet aggregation, thrombosis formation, or intimal hyperplasia. In 2018, Catalano et al. [79] analyzed laser cutting parameters for pure Zn expandable flat geometry stents. The main insights from his work are: i) pure Zn shows at high average power levels a distinct irregular cutting region and an excess of dross is generated, including an unprecise kerf geometry; ii) pure Zn is unable to resist well the chemical etching phase with aqueous HNO3 solutions due to thickness reduction, and iii) a complex mesh geometry made the etching process more difficult. Most importantly, a planar mesh may be expanded using a commercial biomedical catheter to analyze the material's mechanical and biological performance. In 2019, stents with 5 mm in diameter and 20 mm in length with a strut thickness of about 76 μm to 127 μm produced using laser cutting followed by chemical polishing were produced from Zn with 0.8 Cu wt.% addition [80]. They were implanted in Shanghai white pigs in the left anterior descending artery, left circumflex artery, or right coronary artery for 3, 6, 9, 12, 18, and 24 months. At the end of the experiment, the degradation rate was approximately  $28 \pm 13\%$  of the stent remained. It was observed that normal tissue can replace the strut over time without the risk of entering the circulatory system. Thrombosis, localized necrosis, or serious inflammatory responses were not found after 24 months experiment [80]. During the same year, Lin et al. [81] developed Zn-0.02Mg-0.02Cu stents implanted in white rabbits in their left carotid artery for 24 months. After a week, stents showed rapid endothelization, indicating a low cytotoxicity and thrombosis risk. After implantation, the release of Zn<sup>2+</sup> ions was measured in different organs and serums from the rabbits. It was observed that Zn<sup>2+</sup> concentrations were not significantly different between the stented and the control group of rabbits; Mg<sup>2+</sup> and

Cu<sup>2+</sup> were not absorbed into the organs due to their trace content in the alloy. This research showed that Zn-0.02Mg-0.02Cu stent maintains its mechanical integrity for up to 6 months (showing a corrosion rate of about 25 μm/year). The corrosion rate was accelerated after 12 months of implantation (increasing to 40 μm/year), leading to stent fragmentation and brittleness. In 2020, Zhou et al. [82] studied Zn-0.8Cu (wt.%) stents with polymer (D, L-lactide-co-glycolide) and Sirolimus coating. The mechanical properties and restoration of the vessel after in vivo studies in porcine coronary arteries had low mechanical strength (yield strength ~111 MPa, ultimate tensile strength ~142 MPa, and elongation ~193%) that resulted in reduced radial strength, also a lower bending force that would be beneficial for long stents flexibility. In 2022, the stents prepared from Zn-2.0Cu-0.5Mn with a size of ~2.83 mm in diameter and 16 mm in length and a strut thickness of about 125 µm were investigated by Jiang et al. [83]. Samples were analyzed by in vitro techniques such as electrochemical and immersion tests in C-SBF, the latter one lasted for 480 h. It was observed that the corrosion rate was about 158 µm/year with a uniform corrosion morphology with small corrosion pits formed (~2-3 μm). Two years later, Qian et al. [84] evaluated the Zn-2.0Cu-0.5Mn alloy to understand biosafety and biodegradability through in vivo tests using porcine coronary arteries. The results indicated that an optimal endothelization after 1 month, the degradation rate was desirable while its basic structure and mechanical properties could maintain integrity 6 months after implantation. The implanted stent was almost degraded at 18 months, with 26% stent volume remaining.

Recently, Zhang et al. [85] studied the influence of Li on Zn-2Cu alloys by adding 0.004, 0.01, and 0.07 Li (wt.%). They fabricated stents from Zn-2Cu-0.07Li and investigated mechanical, corrosive, and cytocompatibility properties. The best properties observed were after adding 0.07 Li (wt.%), whose mechanical properties yield tensile strength >320 MPa, ultimate tensile strength >360 MPa, and elongation ~28%. The corrosion rate shown for Zn-2Cu-0.07Li was ~90  $\mu$ m/year, higher than that calculated for the Zn-2Cu alloy (~75  $\mu$ m/year). The cytocompatibility was analyzed using human umbilical vein endothelial cells (HUVEC) with 10% and 50% extracts after 1, 3, and 5 days of immersion. It showed above 90% cell viability for 10% extracts after all-time points tested and after 1 and 3 days in 50% extracts.

#### 4.4. Photo-chemical etching

Photo-chemical etching is a simple and inexpensive process that can form the texture of a stent [86]. Photo-chemical etching uses photoresists and etchants to chemically remove material from sheets or tubes to produce high-resolution complex designs [49]. It has been proven suitable for machining stents with photolithography to transfer a selected stent pattern into a flat metal sheet [86]. Kandala et al. [87] used photo-chemical etching to fabricate rhombus, U, and omega shapes of stents from pure Zn (Fig. 3). Compression tests recorded in loading and unloading mode indicated that the rhombus design stent had a maximum value of 0.167 N/mm radial force over stent length.

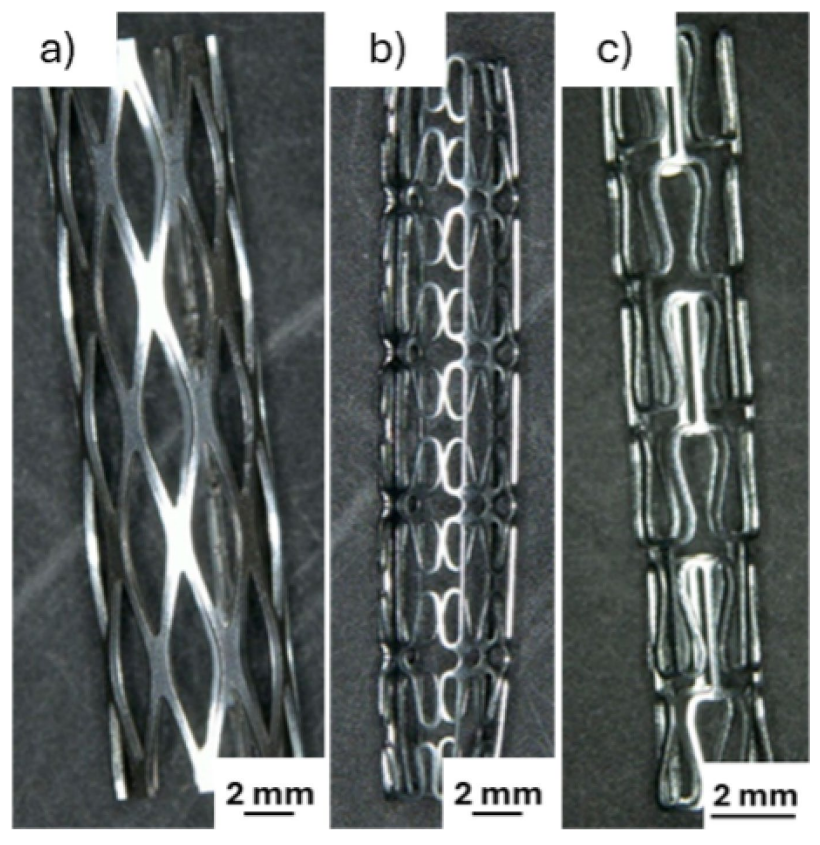


Fig. 3. Pictures of Zn stents produced using photo-chemical etching with different designs: a) rhombus, b) U-design, and c) omega design. Images from Kandala et al. [87]. Open access article distributed under the Creative Common Attribution License

In contrast, U and omega design stents obtained 0.25 N/mm and 0.07 N/mm, respectively. Due to the intermediate compression value for the rhombus design stent, Parylene C coating was applied and investigated for this stent. It was found that exposed rhombus-shaped samples had a smooth and uniform expansion with and without Parylene C coating. In the case of in vitro results, it was observed that the corrosion rate of unexpanded, uncoated stents was around 0.0951 mm/year; the addition of Parylene C coating showed a 50% reduction in corrosion rates for unexpanded stents and a 25% reduction for the expanded stent that may be related to the elastoplastic deformation. Additionally, in vivo results showed that the Zn ribbons implanted subcutaneously in C57Bl/6 mice were intact with less degraded parts than AZ31 Mg samples. Histological studies showed that Zn produced a slightly more inflammatory response, but no necrotic tissue was observed. However, Zn did not irritate the blood vessels as these approached the metal without an inflammatory reaction around it.

#### 4.5. Additive manufacturing

AM is a layer-by-layer manufacturing method that is different from the traditional subtractive manufacturing process. AM, also known as 3D printing, provides opportunities to produce personalized designs according to the patient-specific that can meet exact requirements due to its excellent geometric freedom and dimensional accuracy, making it suitable for manufacturing complex structures [88]. Since it has been demonstrated that stent design features are of great importance for a successful treatment due to correlations with thrombosis and in-restenosis risk, obtaining the proper shape of stents is crucial [16]. Unfortunately, Zn is hard to process using AM because of its high evaporation due to the long-time laser melting process that may lead to the formation of severe spatter and porous structures [89]. To avoid such complications an optimized gas circulation system should be used to help to get rid of Zn metal vapor inside the chamber and prevent oxidation or other harmful gas intrusion [90]. Nevertheless, in 2017, Montani et al. [91] investigated pure Zn produced using selective laser melting (SLM). They found that Zn shows less processability due to its low vaporization point, which leads to the formation of significant porosity during the processing. They obtained samples with high porosity levels (~12%); although the sample was porous, it showed higher mechanical strength than cast Zn. In 2018, using SLM, Wen et al. [92] obtained highly dense (over 99.90%) pure Zn. In the same year, Wen et al. [93] studied the mechanical properties of 3D printed pieces and showed elastic modulus (23 GPa), yield strength (114 MPa), ultimate strength (134 MPa), and elongation (10.1%). Overall, tensile properties were better than values obtained for pure Zn produced by casting, hot rolling, and hot extrusion. Based on the optimization parameters performed for bulk material, they attempted to print stents; however, their mechanical and degradation properties were not investigated.

In 2019, Wen et al. [90] described the key parameters for

printing Zn solid cubes with high density (99.8%). They used laser power of 80 W, scanning speed of 400 mm/s, hatch spacing of 70  $\mu$ m, layer thickness of 30  $\mu$ m, spot diameter of 75  $\mu$ m, and 0 mm for defocus distance. The average grain size observed was in width 8.5  $\mu$ m while the microhardness Vickers obtained was about 43 HV. In 2022, Voshage et al. [94] produced Zn-xMg (x = 0, 1, 2 and 5 wt.%) alloys laser powder bed fusion (LPBF), obtaining greater relative densities than 99.5 % and found that the Zn-xMg alloys had a smaller processing window due to the different melting temperatures after the addition of Mg. The printed alloy had a tensile strength of 381 MPa and elongation of 4.2%, higher than pure Zn.

# 5. Zn microstructure after various manufacturing techniques: emphasis on additive manufacturing

Zn and its alloys show different microstructures, depending not just on the alloy's chemical composition but also on the manufacturing process. For example, after the laser cutting procedure, the final microstructure has shown no significant thermal effects or generated grain growth. Also, the texture orientation was not modified [26]. This would lead to the possibility of changing the microstructure during the casting, extrusion, rolling, or drawing processes; for example, Wang et al. [72] studied rolled and drawn micro-tubes and found that fine and homogeneous microstructure can be controlled from ~6 μm to up to ~20 mm mean grain size after cold forming from the rolling, drawing, and posterior annealing method. Dai et al. [73] studied Zn tubes with the addition of 0.5 wt.% Li. It was found that uniform, regular equiaxed grains of about 10 µm were obtained after the extrusion process. This could be related to the Li content that produced small LiZn<sub>4</sub> secondary particles that allowed the formation of refined grains of about 200 nm to up to 2 µm. Jin et al. [68] studied cast, extruded, and drawn Zn wires with the addition of 0.002, 0.005, and 0.08 (wt.%) Mg. They found that the grain size was reduced with increasing Mg content after obtaining  $\sim 76 \, \mu m$ for Zn-0.002 Mg, and  $\sim$ 7 µm and  $\sim$ 8 µm, respectively, for 0.005 and 0.08 Mg. Jiang et al. [83] studied as-extruded and as-drawn tubes of Zn-2.0Cu-0.5Mn (wt.%) with an average grain size of  $\sim$ 2 µm with the apparition of CuZn<sub>4</sub> and MnZn<sub>13</sub> phases. After the laser cutting and electropolishing processes, it was found that the microstructure of the stents was not affected. Ren et al. [74] investigated the properties of Zn-0.1Mg01Mn (wt.%) tubes at different extrusion temperatures. It was observed that for 100°C, 200°C, and 300°C extrusion temperatures, the average grain size changed from  $\sim 1~\mu m$  to  $\sim 1.5~\mu m$  and  $\sim 1.9~\mu m$ , respectively. Lou et al. [75] studied tubes of Zn-0.5Mn-0.05Mg (wt.%) after 2 and 5 passes during rolling at ambient temperature. It was observed that the average grain size decreased after 2-pass rolling from  $\sim$ 1.6  $\mu$ m for as-extruded samples to  $\sim$ 0.9  $\mu$ m. Also, it was found that a more uniform grain size appeared after the 5-pass rolling process that increased strength due to the texture evolution and a change in the dominant deformation mechanism from twinning and dislocation movement to solely dislocation

movement for 2 and 5 passes rolling, respectively. Zhang et al. [85] studied the influence of the 0.004, 0.01, and 0.07 (wt.%) addition of Li in Zn-2Cu. It was observed that the microstructure is composed of fine equiaxed  $\eta$ -Zn grains and  $\epsilon$ -CuZn<sub>4</sub> phases in micron, submicron, and nano-sized. After adding Li, the grain size distribution became more uniform with refined grains due to the increasing volume fraction of submicron and nano-sized  $\epsilon$ -CuZn<sub>4</sub> precipitates. The average grain size obtained is  $\sim$ 4.8  $\mu$ m,  $\sim$ 2.9  $\mu$ m, and  $\sim$ 1.9  $\mu$ m, respectively, for 0.004, 0.01, and 0.07 (wt.%) addition of Li.

Several studies have been made to understand the relationship between additive manufacturing parameters and the microstructure obtained. For example, Wen et al. [92] obtained fine columnar grains with epitaxial growth along the building direction in SLM-deposited layers of pure Zn [92]. Another example is when Ning et al. [95] studied pure Zn and Zn-3Mg (wt.%) prepared using SLM. Principally, it was found that adding Mg decreased the average grain size from ~21  $\mu m$  to ~2  $\mu m$ , as shown in Fig. 3a and 3b. But more interesting, it was appreciated that pure Zn contained fine columnar grains growing following the construction direction, as seen in Fig. 4c and 4d. This can be explained by the gradient temperature during the SLM process; rapid melting consequently leads to the powder's solidification, leading to the growth of grains between the deposited layers.

Qin et al. [96] studied the relationship between the effect of grain structure in both mechanical and corrosive properties of printed pure Zn. They observed that the corrosion rate increased with the increasing scanning speed (the decreasing grain size).

Wang et al. [97] compared the cast pure Zn, which was composed of coarse α-Zn grains (size of several hundreds of microns), and SLMed material that showed finer equiaxed grains (~8 µm). This type of grain was explained due to the low-temperature gradient and high scanning speed. Also, lamellar structures were observed, located inside some equiaxed grains. They mostly appeared parallel to the deposition direction with a 99.84% Zn and 0.16% O composition. However, O was highly concentrated at the grain boundaries (~15 wt.%). In addition, the volume energy (E<sub>v</sub>) was studied to understand the grain size and ZnO volume; it was shown that the increase in E<sub>v</sub> did not increase the ZnO. However, the grain size increased from  $\sim$ 8 µm to  $\sim$ 9.5 µm. Also, high scanning speed (V) and low laser power (P) produced a low E<sub>v</sub>, leading to powder accumulation that could not melt completely. Nonetheless, the final samples obtained were 93% dense with optimized parameters: hatch spacing = 70 µm, layer thickness = 30  $\mu$ m, volume energy = 83.33-158.73 J/mm<sup>3</sup> [97]. In 2021, Qin et al. [98] explained that it is difficult to maintain low evaporation and enough melting properties of Zn when using a high laser power and high scanning speed that could not produce densification [98]. In 2023, Yang et al. [99] obtained highly dense Zn samples (over 99.5%) and studied the relationship between LPBF parameters, crystal orientation, and texture. They reported that a power of 80 W and speed of 400 mm/s produce mainly grains oriented towards <0001> with a strong texture. The increase in speed supports the formation of fine grains, and texture weakening is observed. Also, the increasing speed enhances strength and ductility. The most recent research

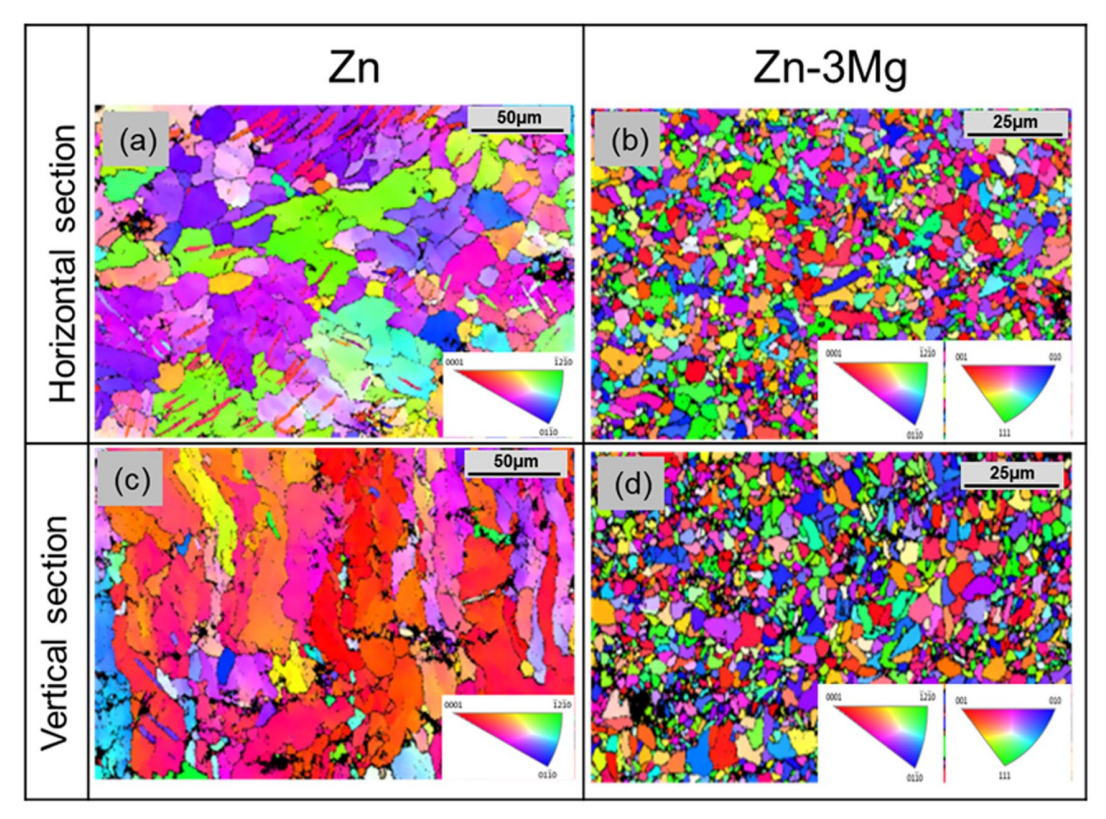


Fig. 4. EBSD results for pure Zn and Zn-3Mg (wt.%) after SLM processing: a) horizontal section for pure Zn, b) horizontal section for Zn-3Mg, c) vertical section for pure Zn, and d) vertical section for Zn-3Mg. Image from Ning et al. [95]. Open access article distributed under the Creative Common Attribution License

on pure Zn produced using LPBF was made by Dong et al. [100]. The printed pure Zn exhibited anisotropy along horizontal and vertical planes, obtaining fine equiaxed grains of about 9.63 µm that showed better strength and ductility synergy performance than traditionally cast Zn. They proved that the horizontal planes have enhanced pre-existing dislocations that support the formation of a stable and flat passive film on the surface, which helped to delay the corrosion processes [100]. In 2023, Waqas et al. [101] studied pure Zn and Zn-10Mg alloys produced using SLM. They found that the apparition of pores resulted from poor fusion with unfused powder [101]. An important discovery related to the building direction during the SLM process was made in 2024 by Li et al. [102] who fabricated Zn-0.8Cu (wt.%) alloy focusing on vertical and horizontal printing directions. The obtained samples had a relative density beyond 99.5%. The authors expected that the corrosion resistance would increase by incorporating Cu in the Zn matrix. However, a small amount of Cu did not show strong diffraction peaks during XRD analysis, nor were Cu compounds found in the corrosion products. They supposed that CuZn<sub>5</sub> precipitates formed at grain boundaries could easily form localized corrosion, making the alloy less resistant than pure Zn [102].

As shown in this review, the AM used for Zn and its alloys is very limited; however, since it shows promising opportunities, it should be widely expanded. AM is one of the best opportunities to print complicated shapes of stents and allows to achieve the desired qualities for biodegradable stents applications [103]. The comparison of various methods, their parameters, and results of microstructure, mechanical, corrosion, and biological properties on Zn alloys performed during the last decade is shown in TABLE 1.

#### 6. Summary

Zn is a promising metal for temporary cardiovascular stents, not just because of its optimal biocompatibility and biodegradability, but also because it is essential for the human body. However, its mechanical performance is still being investigated to fulfill temporary stenting requirements. Currently, various manufacturing methods have been used to produce cardiovascular stents, including casting, extrusion, rolling, tube drawing, and laser cutting, which are used to produce Zn stents. Early research on Zn and its alloys for temporary stents focused on simplified geometries like wires and tubes. These studies provided essential data, especially on degradation properties. The performed literature review clearly shows that stent degradation strongly depends on the strut size. Hence, the simplified geometry of wires and tubes presents limitations to understanding due to the lack of accurately replicating the fluid dynamics and mechanical behavior expected in a stent within a vessel. Consequently, the findings from early studies are informative. However, they cannot fully predict in vivo performance. This requires moving towards manufacturing processes for Zn to mimic stent geometries that are already used for clinical usage. For this reason,

more advanced investigations have been dedicated to producing Zn stents using laser cutting. Laser cutting provides a similar stent shape and size that helps understand the mechanical and degradation properties and have closer insights related to the degradation and corrosion mechanism during *in vitro* and *in vivo* tests. Mechanical properties are also influenceable as they vary before and after balloon catheter expansion. Also, biological properties can be nearby study with direct interaction with the endothelization processes. Therefore, new ways to produce stents have been considered; for example, one study was dedicated to photo-chemical etching as an alternative to laser cutting.

Moreover, new technologies have emerged, creating a unique manufacturing path for producing cardiovascular stents. Additive manufacturing has gained interest due to its possibility of obtaining personalized designs that can match patient needs through freedom for complex design and the accuracy it can provide. The greatest challenge for 3D printing using Zn and its alloys is the lack of processability due to its high evaporation in the long-time laser melting process that produces highly porous structures. The last studies showed improved porosity levels of Zn with highly dense structures (~99%) by managing the printing parameters. It was reported that the modification in processing parameters can produce changes in the microstructure and texture of the final product in comparison with laser cutting, which commonly minimizes thermal effects and microstructure modifications.

The application of AM to Zn and its alloys has shown promise in enhancing mechanical performance compared to traditional production routes. This is not solely related to the chemical composition but also due to the unique microstructures and textures created during AM. Therefore, further investigation should be done to ensure the long-term safety and efficacy of using 3D-printed Zn-based stents. Moreover, it should move from simple samples to complex-shaped stent geometries, which remain crucial for further research.

#### 7. Conclusions

This review has highlighted the current progress, challenges, and opportunities of Zn-based biodegradable cardio-vascular stents. Zn and its alloys have demonstrated potential as a material for biodegradable cardiovascular stents. Zn has been considered as an alternative to Mg- and Fe-based systems due to its favorable degradation rate, which avoids adverse effects as hydrogen release or corrosion residues. However, its lack of mechanical performance is still a matter of study.

The central insight from this review is how manufacturing techniques from conventional approaches to new emerging technologies, such as additive manufacturing, are playing an important role in shaping the microstructure, mechanical integrity, degradation performance, and biocompatibility. A key conclusion is that the control of microstructure is essential for Zn-based stents; features as grain size, texture, and second-phase dispersion are essential to enhance strength and degradation. Additive

Zn and its alloys investigated for bioresorbable cardiovascular stenting applications within various manufacturing techniques

TABLE 1

Grain size	11		For rolled tubes:  -6 µm  For drawn tubes after annealing:  -20 µm	l	I	l	-5.6 µm	~10 $\mu$ m with refined grains of about ~200 nm to ~2 $\mu$ m	~76 µm	m⊭ /~	шт 9~
Mechanical properties	10	Tensile strength $-44.50 \pm 1.76$ MPa Elongation $-7.57 \pm 0.20\%$	For micro-tubes UTS $-> 220$ MPa YS $-120$ MPa Elongation $-> 20\%$	I	UTS $-274 \pm 61$ MPa YS $-238 \pm 60$ MPa Elongation $-17 \pm 7\%$ Hardness $-97 \pm 2$ Hv		For cube printed samples Hardness – ~42 Hv YS – ~115 MPa Average ultimate strength – ~130 MPa Elongation – 7% – 12%	UTS – 296.2 MPa Elongation 33%	Zn-0.002 Mg YS – 34 ± 4 MPa Tensile strength – 63 ± 9 MPa Elongation – 17 ± 3% Hardness – 45 Hv	Zn-0.005 Mg YS $- 93 \pm 1$ MPa Tensile strength $- 202 \pm 60$ MPa Elongation $- 28 \pm 2\%$ Hardness $- 93 \pm 1$ Hv	Zn-0.8Mg YS -> 200 - 300 MPa Tensile strength -> 300 - 400 MPa Elongation -> 30% Hardness - 103 ± 1 Hv
Degradation rate	6	~0.028 to 0.037 mm/year	0.062 mm/year for drawn micro-tubes 0.040 mm/year for rolled micro-tubes	$41.75 \pm 29.72\%$ stent volume after 12 months	0.008 mm/year for 2 months 0.045 mm/year for 12 months	l	l	l	1.5 months $\sim$ 0.029 mm/year 11 months $\sim$ 0.05 mm/year	1.5 months $\sim 0.021$ mm/year 11 months $\sim 0.03$ mm/year	1.5 – 4 months degradation rate ~ 0.027 mm/year 6 – 11 months ~0.023 mm/year
in vivo	8	ı	I	Abdominal aortas of Japanese rabbits for 12 months	Abdominal aorta of Sprague- Dawley rats for 2 and 12 months.	I	I	I	Abdominal aorta of Sprague- Dawley rats for 1.5, 3, 4.5, 6 and 11 months	Abdominal aorta of Sprague- Dawley rats for 1.5, 3, 4.5, 6 and 11 months	Abdominal aorta of Sprague- Dawley rats for 1.5, 3, 4.5, 6 and 11 months
in vitro	7	HBSS for 250 h	SBF for 48 days	l	I	l	l	l	I	I	I
Strut/ thickness size	9	0.15 mm thickness	130 mm thickness.	165 µm	l	~100 µm	500, 300, 300 and 200 µm respectively.	I		l	I
Size	5	2 mm outer diameter	2.5 mm diameter	3 mm diameter and 10 mm length	0.25 mm diameter and 2 cm length	Novel flat stent: 11 mm length	5-, 4-, 3- and 2-mm diameters	1.5 mm diameter and 0.13 mm thickness	0.25 mm diameter and 15 mm length	0.25 mm diameter and 15 mm length	0.25 mm diameter and 15 mm length
Shape	4	Tubes and plates	Tubes	Stents	Wires	Stents	Stents, cubes and cylinders	Tubes	Wires	Wires	Wires
Manufacturing process	3	Extrusion, drawing and electrochemical polishing	Cast, extrusion, drilling, rolling, mandrel drawing, annealing, laser etching and electrochemical polishing	Laser cutting and electrochemical polishing	Casting by induction melting, extrusion, drawing and polish (diamond and alumina slurry)	Laser micro cutting, chemical etching with HNO <sub>3</sub> solution	Nitrogen atomized pure Zn powder, selective laser melting and sandblasting	Gravity casting, quenching, hot extrusion and drawing	Casting, extrusion and drawing	Casting, extrusion and drawing	Casting, extrusion and drawing
Year	2	2015	2016	2017	2017	2018	2018	2018	2018	2018	2018
Composition	1	Ultra-pure Zn [71]	Zn-5Mg-1Fe (wt.%) [72]	Pure Zn [78]	Zn-0.1Li (wt.%) [67]	Pure Zn [79]	Pure Zn [93]	Zn-0.5Li (wt.%) [73]	Zn-0.002Mg (wt.%) [68]	Zn-0.005Mg (wt.%) [68]	Zn-0.08Mg (wt.%) [68]

11					I	
10	Rhombus design – 0.167 N/mm radial force (compression after ballon expanding over stent length) U design – 0.25 N/mm and Omega design – 0.07 N/mm	I	Radial strength – 114 ± 3 kPa	TYS – 216.29 $\pm$ 3.27 MPa UTS – 262.25 $\pm$ 5.02 MPa Hardness – 74.40 $\pm$ 1.84 Hv Elongation – 27.74 $\pm$ 2.21%	Maximum push force – 1.21 ± 0.09 N Intrinsic elastic recoil – 0.41 ± 0.18 % Bending force – 0.14 ± 0.02 N Radial strength 112.60 ± 3.18 kPa YS – 111.0 ± 4.9 MPa UTS – 142.7 ± 9.2 Elongation – 193.8 ± 2.5% Young's modulus – 89.10 ± 6.26	
6	Unexpanded uncoated Zn stents – 0.0951 mm/ year and Parylene C-coated with 50% reduction.	Based on electrochemical results For electropolished sample – 0.26 ± 0.03 mm/year For anodized sample – 0.32 ± 0.01 mm/year	Residual volume 3 months – 92 ± 1% 6 months – 79 ± 4% 9 months – 77 ± 4 4% 12 months – 74 ± 12% 18 months – 56 ± 19% 24 months 28 ± 13%	Penetration rate for 3-6 months $-25 \mu$ 12 months $-$ v38.76 $\pm$ 13.17 $\mu m$	I	
8	Subcutaneous implantation in C57BL/6 mice for 15 days	Aortic lumen of Sprague-Dawley rats for 2, 4 and 8 weeks	Left anterior descending artery (LAD), left circumflex artery (LCX) or right coronary artery (RCA) of Shanghai white pigs for 24 months	White rabbits in left carotid artery for 12 months	Porcine coronary artery for 18 months	
7	DMEM + 10% FBS + 1% P/S for 72 h.	HBSS for 28 days	I	I	I	
9	l		76 µm to 127 µm	~130 µт	Structural thickness 0.127 mm	
2	Designs: Rhombus 4 mm diameter U 7.4 mm, Omega 5.68 mm and 6.20 mm outer diameter Length of 19.5 mm - thombus (design) 25 mm - U (design) 25 mm - Omega (design)	0.25 mm wires and 8 mm diameter discs	5 mm diameter and 20 mm length	2 mm diameter and 12 mm	3 mm outer diameter and 20 mm length	
4	Stents	Wires and discs	Stents	Tubes	Stents	
3	Photo-chemical etching Rhombus designed stents were coated with polymer Parylene C sublimation in a Physical Vapor Deposition (PVD)	Electropolish and anodized	Femtosecond-laser cutting, acid pickling and chemical polishing	Drilling, rolling, cold mandrel drawing and intermediate annealing method, laser cutting and electrochemical polishing	Casting, drawing and laser cutting. Additionally, spray coated with the polymer/ sirolimus coating matrix using poly (D. L-lactide-co-glycolide)	
2	2019	2019	2019	2019	2020	
1	Pure Zn [87]	Pure Zn [69]	Zn-0.8Cu (wt.%) [80]	Zn-0.02Mg- 0.02Cu [81]	Zn-0.8Cu (wt.%) [82]	

11	~2 µm	100 °C ~1 µm 200 °C ~1.5 µm 300 °C ~1.9 µm	mu [~	ı	~4.8 µm	~2.9 µm	mµ 6.1∽
10	As-drawn tube  UTS $- 298 \pm 3$ MPa  YS $232 \pm 3$ MPa and elongation $26 \pm 1\%$ .  For laser cut stent  Radial strength $- 150 \pm 10$ kPa  Recoil $- 2.5 \pm 0.8\%$ Foreshortening $- 1.5 \pm 0.8\%$	After 100 °C UTS – 405 MPa YS – 380 MPa CYS – 428 MPa Elongation – 14% After 200 °C UTS – 395 MPa YS – 377 MPa CYS – 380 MPa Elongation – 11.2% After 300 °C UTS – 340 MPa YS – 340 MPa CYS – 290 °C Elongation – 5.5%	YTS – 277 $\pm$ 2.9 MPa UTS – 330 $\pm$ 3.3 MPa Elongation – 39.8 $\pm$ 5.25%	I	For as extruded samples: TYS $\sim$ 214 MPa UTS $\sim$ 262 MPa Elongation - $\sim$ 28%	For as extruded samples: $TYS - \sim 266 \text{ MPa}$ $UTS - \sim 326 \text{ MPa}$ Elongation - $\sim 26\%$	For as extruded samples: TYS - ~300 MPa UTS - ~360 MPa Elongation - ~30%
6	158 µm/year for as-drawn tube	I	I	Residual volume 3 months – ~90.6 % 6 months – ~74.4% 12 months – ~50% 18 months – ~26%	I	I	For as-extruded samples 89.5 ± 6.6 μm/year
80		l	I	Implanted into porcine coronary artery for 1, 3, 6, 12 and 18 months	l	I	-
7	C-SBF at 37°C for 480 h	I		I			c-SBF for 21 days
9	Structural thickness ~125 µm	2 mm		I	0.16 mm	0.16 mm	0.16 mm
ĸ	~2.83 mm diameter and 16 mm length	12 mm outer diameter	3.5 outer diameter and 0.2 mm thickness	3 mm outer diameter and length of 16 mm	3 mm outer diameter and 16 mm in length	3 mm outer diameter and 16 mm in length	3 mm outer diameter and 16 mm in length
4	Stents and tubes	Tubes	Tubes	Stents	Stents and tubes	Stents and tubes	Stents, rods and tubes
8	Gravity casting and homogenization treatment, extrusion, preheating, drawing, femtosecond-laser cutting and electrochemical polishing (electrolyte of 35% phosphoric acid, 10% acetic acid, 55% glycol at 50°C)	Water-cooled iron casting method, homogenizing treatment and multi- forged, drilled and indirectly extrusion	Casting, heat-treat, die forging and inter annealing Indirect extrusion with mandrel and rolling	Gravity casting, homogenization treatment, extrusion, drawing, femtosecond laser cutting and electropolishing	Casting, extrusion, two-pass drawing, femtosecond laser and electrochemical polishing	Casting, extrusion, two-pass drawing, femtosecond laser and electrochemical polishing	Casting, extrusion, two-pass drawing, femtosecond laser and electrochemical polishing
2	2022	2022	2024	2024	2024	2024	2024
1	Zn-2.0Cu- 0.5Mn (wt.%) [83]	Zn-0.1Mg- 1Mn (wt.%) [74]	Zn-0.5Mn- 0.05Mg (wt.%) [75]	Zn-2Cu-0.5Mn (wt.%) [84]	Zn-2Cu- 0.004Li (wt.%) [85]	Zn-2Cu-0.01Li (wt.%) [85]	Zn-2Cu-0.07Li (wt.%) [85]

manufacturing, in particular, introduces unique microstructures that may enhance mechanical integrity, but the process remains challenging due to Zn's low processability.

The review also reveals a major limitation in research studies, as the use of simplified geometries, such as wires or tubes, which do not accurately represent the mechanical behavior or fluid dynamics of a deployed stent. Transition to real stent geometries, especially through laser cutting and additive manufacturing, is introducing new challenges in formability, mechanical integrity, and degradation performance, which is essential to bring the field closer to clinical studies.

In general, Zn and Zn alloys represent a promising material for biodegradable cardiovascular stents, but it has challenges in mechanical performance, long-term stability, and geometry-specific behavior that must be addressed.

#### 8. Prospectives

This review has highlighted the attention to Zn as a potential material for temporary cardiovascular stents. Zn and its alloys are biocompatible and biodegradable; however, their antibacterial properties and mechanical performance still need to be optimized. While significant progress has been made in understanding the material's performance produced using various manufacturing methods, several key areas require further investigation. The following prospectives should be considered:

- Optimization of additive manufacturing parameters: AM has shown enhancement in the mechanical properties of Zn; however, further research is needed to optimize the process for fabricating diverse stent shapes and sizes. Furthermore, systematic studies are required to comprehend the influence of AM process parameters on corrosion behavior and how it affects the biocompatibility of Zn stents. An essential step will be to characterize the microstructural, mechanical, corrosive, and biological properties of Zn after they have been subjected to balloon catheter expansion, which is an important part that may alter the stent structure.
- Alloying to enhance Zn performance: the current limitations
  of Zn in achieving mechanical properties suggest that alloying can be helpful, especially for its usage in AM, which
  has been poorly investigated among Zn and its alloys.
- Although several studies report mechanical properties of Zn as yield strength, ultimate tensile strength, and elongation, none of them explicitly examined the softening effect and the lack of strain hardening after various manufacturing techniques, especially for cardiovascular stenting applications [104] where a lack of strain hardening during balloon expansion of stents may produce a non-uniform deployment and easily lead to an immediate recoil [105]. This represents a critical knowledge gap since these effects are directly connected to the stent deployment and stability during the healing treatment. Therefore, future research should focus on understanding the relationship between processing routes with the microstructure and deformation mechanisms to

- better predict and optimize the mechanical functionality, specifically in cardiovascular stents.
- Long-term in vitro and in vivo performance: comprehensive studies are needed to assess the long-term efficacy and safety of Zn and its alloys after AM processing.

By understanding and addressing these key research gaps, the Zn field can move closer to understanding its potential as a material for temporary cardiovascular stents, which offer a promising alternative to current cardiovascular stents, permanent metallic or temporal bioresorbable polymers.

#### Acknowledgments

This research was funded by a subvention for statutory activities at the Faculty of Materials Science and Engineering, Warsaw University of Technology, Poland.

Marlene Aydee Gonzalez Garcia thanks Secretaría de Ciencia, Humanidades, Tecnología e Innovación (Spanish for Secretariat of Science, Humanities, Technology, and Innovation; abbreviated SECIHTI) for the support provided as a scholarship for studying abroad.

#### REFERENCES

- [1] A.K. Malakar, D. Choudhury, B. Halder, P. Paul, A. Uddin, S. Chakraborty, A review on coronary artery disease, its risk factors, and therapeutics. J. Cell. Physiol. 234, 16812-16823 (2019). DOI: https://doi.org/10.1002/jep.28350
- [2] K. Okrainec, D.K. Banerjee, M.J. Eisenberg, Coronary artery disease in the developing world. Am. Heart. J. 148, 7-15 (2004). DOI: https://doi.org/10.1016/j.ahj.2003.11.027
- [3] B. Chong, J. Jayabaskaran, S.M. Jauhari, S.P. Chan, R. Goh, M.T.W. Kueh, et al., Global burden of cardiovascular diseases: projections from 2025 to 2050. Eur. J. Prev. Cardiol. (2024). DOI: https://doi.org/10.1093/eurjpc/zwae281
- [4] Global Effect of Cardiovascular Risk Factors on Lifetime Estimates. N. Engl. J. Med. (2025).
  DOI:https://doi.org/10.1056/nejmoa2415879
- [5] A. Scafa Udrişte, A.G. Niculescu, A.M. Grumezescu, E. Bădilă, Cardiovascular stents: A review of past, current, and emerging devices. Materials. 14 (10), 2498 (2021). DOI: https://doi.org/10.3390/ma14102498
- [6] A. Das, S. Mehrotra, A. Kumar, Advances in Fabrication Technologies for the Development of Next-Generation Cardiovascular Stents. J. Funct. Biomater. 14 (11), 544 (2023).
  DOI: https://doi.org/10.3390/jfb14110544
- [7] P.K. Bowen, E.R. Shearier, S. Zhao, R.J. Guillory, F. Zhao, J. Goldman, et al., Biodegradable Metals for Cardiovascular Stents: from Clinical Concerns to Recent Zn-Alloys. Adv. Healthc Mater. 5, 1121-1140 (2016).
  - DOI: https://doi.org/10.1002/adhm.201501019
- [8] C.S. Bruikman, R.M. Stoekenbroek, G.K. Hovingh, J.P. Kastelein, New Drugs for Atherosclerosis. Can. J. Cardiol. 33, 350-357 (2017). DOI: https://doi.org/10.1016/j.cjca.2016.09.010

- [9] L.A.G. Rodríguez, M. Martín-Pérez, C.H. Hennekens, P.M. Rothwell, A. Lanas, Bleeding risk with long-term low-dose aspirin: A systematic review of observational studies. PLoS. One. 11, 1-20 (2016).
  - DOI: https://doi.org/10.1371/journal.pone.0160046
- [10] M.B. Elam, G. Majumdar, K. Mozhui, I.C. Gerling, S.R. Vera, H. Fish-Trotter, et al., Patients experiencing statin-induced myalgia exhibit a unique program of skeletal muscle gene expression following statin re-challenge. PLoS. One. 12, 1-26 (2017). DOI: https://doi.org/10.1371/journal.pone.0181308
- [11] R.H. Goetz, M. Rohman, J.D. Haller, R. Dee, S.S. Rosenak, Internal Mammary-Coronary Artery Anastomosis. J. Thorac. Cardiov. Sur. 41, 378-386 (1961).
  DOI: https://doi.org/10.1016/s0022-5223(20)31701-3
- [12] N. Korei, A. Solouk, M.H. Nazarpak, A. Nouri, A review on design characteristics and fabrication methods of metallic cardiovascular stents. Mater. Today. Commun. 31, 103467 (2022). DOI: https://doi.org/10.1016/j.mtcomm.2022.103467
- [13] T. Gour, A. Ayoola, Treatment Options for High Cardiometabolic Risk Patients with Atherosclerosis. J. Student. Res. 12, 1-13 (2023).
   DOI: https://doi.org/10.47611/jsrhs.v12i4.5529
- [14] S. Borhani, S. Hassanajili, S.H. Ahmadi Tafti, S. Rabbani, et al., Cardiovascular stents: overview, evolution, and next generation. Prog. Biomater. 7, 175-205 (2018). DOI: https://doi.org/10.1007/s40204-018-0097-y
- [15] A.R. Grüntzig, Å. Senning, W.E. Siegenthaler, Nonoperative Dilatation of Coronary-Artery Stenosis. N. Engl. J. Med. 301, 61-68 (1979).
  - DOI: https://doi.org/10.1056/nejm197907123010201
- [16] F. Garcia-Villen, F. López-Zárraga, C. Viseras, S. Ruiz-Alonso, F. Al-Hakim, I. Diez-Aldama, et al., Three-dimensional printing as a cutting-edge, versatile and personalizable vascular stent manufacturing procedure: Toward tailor-made medical devices. Int. J. Bioprinting. 9, 219-255 (2022). DOI: https://doi.org/10.18063/IJB.V9I2.664
- [17] J. Venezuela, M.S. Dargusch, The influence of alloying and fabrication techniques on the mechanical properties, biodegradability and biocompatibility of zinc: A comprehensive review. Acta Biomater. 87, 1-40 (2019).
  DOI: https://doi.org/10.1016/j.actbio.2019.01.035
- [18] H. Hermawan, D. Dubé, D. Mantovani, Developments in metallic biodegradable stents. Acta Biomater. 6, 1693-1697 (2010). DOI: https://doi.org/10.1016/j.actbio.2009.10.006
- [19] M. Peuster, P. Wohlsein, M. Brügmann, M. Ehlerding, K. Seidler, C. Fink, et al., A novel approach to temporary stenting: Degradable cardiovascular stents produced from corrodible metal - Results 6-18 months after implantation into New Zealand white rabbits. Heart. 86 (5), 563-569 (2001). DOI: https://doi.org/10.1136/heart.86.5.563
- [20] R. Waksman, R. Pakala, P.K. Kuchulakanti, R. Baffour, D. Hellinga, R. Seabron, et al., Safety and efficacy of bioabsorbable magnesium alloy stents in porcine coronary arteries. Catheter Cardiovasc. Interv. 68, 607-617 (2006).
  DOI: https://doi.org/10.1002/ccd.20727

- [21] P.K. Bowen, J. Drelich, J. Goldman, Zinc exhibits ideal physiological corrosion behavior for bioabsorbable stents. Adv. Mater. 25, 2577-2582 (2013).
  DOI: https://doi.org/10.1002/adma.201300226
- [22] S.H. Im, D.H. Im, S.J. Park, Y. Jung, D.H. Kim, S.H. Kim, Current status and future direction of metallic and polymeric materials for advanced vascular stents. Prog. Mater. Sci. 126, 100922 (2022). DOI: https://doi.org/10.1016/j.pmatsci.2022.100922
- [23] I. Cockerill, C.W. See, M.L. Young, Y. Wang, D. Zhu, Designing Better Cardiovascular Stent Materials: A Learning Curve. Adv. Funct. Mater. 31, 1-23 (2021). DOI: https://doi.org/10.1002/adfm.202005361
- [24] Y. Li, Y. Shi, Y. Lu, X. Li, J. Zhou, A.A. Zadpoor, et al., Additive manufacturing of vascular stents. Acta. Biomater. **167**, 16-37 (2023). DOI: https://doi.org/10.1016/j.actbio.2023.06.014
- [25] D.W.Y. Toong, J.C.K. Ng, Y. Huang, P.E.H. Wong, H.L. Leo, S.S. Venkatraman, et al., Bioresorbable metals in cardiovascular stents: Material insights and progress. Materialia 12, 100727 (2020). DOI: https://doi.org/10.1016/j.mtla.2020.100727
- [26] E. Mostaed, M. Sikora-Jasinska, A. Mostaed, S. Loffredo, A.G. Demir, B. Previtali, et al., Novel Zn-based alloys for biodegradable stent applications: Design, development and in vitro degradation. J. Mech. Behav. Biomed. Mater. 60, 581-602 (2016). DOI: https://doi.org/10.1016/j.jmbbm.2016.03.018
- [27] N. Beshchasna, M. Saqib, H. Kraskiewicz, Ł. Wasyluk, O. Kuzmin, O.C. Duta, et al., Recent advances in manufacturing innovative stents. Pharmaceutics. 12 (4), 349 (2020). DOI: https://doi.org/10.3390/pharmaceutics12040349
- [28] P. Rola, S. Włodarczak, A. Doroszko, M. Lesiak, A. Włodarczak, The bioresorbable magnesium scaffold (Magmaris) – State of the art: From basic concept to clinical application. Catheter. Cardiovasc. Interv. 100 (6), 1051-1058 (2022). DOI: https://doi.org/10.1002/ccd.30435
- [29] M. Haude, H. Ince, A. Abizaid, R. Toelg, P.A. Lemos, C. Von Birgelen, et al., Safety and performance of the second-generation drug-eluting absorbable metal scaffold in patients with de-novo coronary artery lesions (BIOSOLVE-II): 6 month results of a prospective, multicentre, non-randomised, first-in-man trial. Lancet. 387 (10013), 31-39 (2016).
  - DOI: https://doi.org/10.1016/S0140-6736(15)00447-x
- [30] D. Hernández-Escobar, S. Champagne, H. Yilmazer, B. Dikici, C.J. Boehlert, H. Hermawan, Current status and perspectives of zinc-based absorbable alloys for biomedical applications. Acta. Biomater. 97, 1-22 (2019). DOI: https://doi.org/10.1016/j.actbio.2019.07.034
- [31] H. Tapiero, K.D. Tew, Trace elements in human physiology and pathology: Zinc and metallothioneins. Biomed. Pharmacother. 57 (9), 399-411 (2003).
  DOI: https://doi.org/10.1016/S0753-3322(03)00081-7
- [32] K.A. McCall, C.C. Huang, C.A. Fierke, Function and mechanism of zinc metalloenzymes. J. Nutr. 130 (5), 1437S-1446S (2000). DOI: https://doi.org/10.1093/jn/130.5.1437s
- [33] L. Rink, P. Gabriel, Extracellular and immunological actions of zinc. Biometals. 14, 367-383 (2001).DOI: https://doi.org/10.1023/A:1012986225203

- [34] R.O. Darouiche, Device-Associated Infections: A Macroproblem that Starts with Microadherence. Clin. Infect. Dis. **33** (9), 1567-1573 (2001). DOI: https://doi.org/10.1086/323130
- [35] R.O. Darouiche, Treatment of Infections Associated with Surgical Implants. N. Engl. J. Med. 350 (14), 1422-1429 (2004). DOI: https://doi.org/0.1056/NEJMra035415
- [36] X. Wang, H.M. Lu, X.L. Li, L. Li, Y.F. Zheng, Effect of cooling rate and composition on microstructures and properties of Zn-Mg alloys. Trans. Nonferrous. Met. Soc. China. 17, S122-S125 (2007). Available on website: https://shorturl.at/Xemlz
- [37] T.R. Welch, A.W. Nugent, S.R. Veeram Reddy, Biodegradable Stents for Congenital Heart Disease. Interv. Cardiol. Clin. 8 (1), 81-94 (2019). DOI: https://doi.org/10.1016/j.iccl.2018.08.009
- [38] T. Kogure, S.A. Qureshi, The Future of Paediatric Heart Interventions: Where Will We Be in 2030? Curr. Cardiol. Rep. **22**, 158 (2020). DOI: https://doi.org/10.1007/s11886-020-01404-z
- [39] S.L. Kang, L. Benson, Interventions in Congenital Heart Disease:
   A Review of Recent Developments: Part II. Struct. Heart. 5 (6),
   570-581 (2021).
   DOI: https://doi.org/10.1080/24748706.2021.1990452
- [40] J. Rao, H. Gao, J. Sun, et al., A critical review of biodegradable zinc alloys toward clinical applications. ACS Biomater. Sci. Eng. 10, 5454-5473 (2024). DOI: https://doi.org/10.1021/acsbiomaterials.4c00210
- [41] Y. Zhou, J. Wang, Y. Yang, et al., Laser additive manufacturing of zinc targeting for biomedical application. Int. J. Bioprinting. 8, 74-95 (2022). DOI: https://doi.org/10.18063/IJB.V8I1.501
- [42] Z.Z. Shi, X.X. Gao, H.J. Zhang, et al., Design biodegradable Zn alloys: second phases and their significant influences on alloys properties. Bioact. Mater. 5, 210-218 (2020). DOI: https://doi.org/10.1016/j.bioactmat.2020.02.010
- [43] Z. Wang, J. Song, Y. Peng, New insights and perspectives into biodegradable metals in cardiovascular stents: a mini review. J. Alloys. Compd. 1002, 175313 (2024). DOI: https://doi.org/10.1016/j.jallcom.2024.175313
- [44] I. Limón, J. Bedmar, J.P. Fernández-Hernán, et al., A review of additive manufacturing of biodegradable Fe and Zn alloys for medical implants using laser powder bed fusion (LPBF). Materials. (Basel). 17 (24), 6220 (2024). DOI: https://doi.org/10.3390/ma17246220
- [45] H. Meng, J. Liao, Y. Zhou, Q. Zhang, Laser micro-processing of cardiovascular stent with fiber laser cutting system. Opt. Laser. Technol. 41 (3), 300-302 (2009). DOI: https://doi.org/10.1016/j.optlastec.2008.06.001
- [46] Y. Wu, L. Shen, Q. Wang, L. Ge, J. Xie, X. Hu, et al., Comparison of acute recoil between bioabsorbable poly-L-lactic acid XINSORB stent and metallic stent in porcine model. J. Biomed. Biotechnol. 2012 (1), 413956 (2012).
  DOI: https://doi.org/10.1155/2012/413956
- [47] D. Stoeckel, C. Bonsignore, S. Duda, A survey of stent designs.
   Minim. Invasive. Ther. Allied. Technol. 11 (4), 137-147 (2002).
   DOI: https://doi.org/10.1080/136457002760273340
- [48] D. Pierson, J. Edick, A. Tauscher, E. Pokorney, P. Bowen, J. Gelbaugh, et al., A simplified in vivo approach for evaluating the bioabsorbable behavior of candidate stent materials. J. Biomed.

- Mater. Res. Part. B. Appl. Biomater. **100B** (1), 58-67 (2012). DOI: https://doi.org/10.1002/jbm.b.31922
- [49] A.W. Martinez, E.L. Chaikof, Microfabrication and nanotechnology in stent design. Wiley Interdiscip. Rev. Nanomedicine. Nanobiotechnol. 3 (3), 256-268 (2011). DOI: https://doi.org/10.1002/wnan.123
- [50] Y. Wang, J. Zhan, W. Bian, X. Tang, M. Zeng, Local hemodynamic analysis after coronary stent implantation based on Euler-Lagrange method. J. Biol. Phys. 47, 143-170 (2021). DOI: https://doi.org/10.1007/s10867-021-09571-y
- [51] C. Briguori, C. Sarais, P. Pagnotta, F. Liistro, M. Montorfano, A Chieffo, et al., In-stent restenosis in small coronary arteries: Impact of strut thickness. J. Am. Coll. Cardiol. 40 (3), 403-409 (2002). DOI: https://doi.org/10.1016/S0735-1097(02)01989-7
- [52] Z. Chen, Y. Fan, X. Deng, Z. Xu, A New Way to Reduce Flow Disturbance in Endovascular Stents: A Numerical Study. Artif. Organs. 35 (4), 392-397 (2011). DOI: https://doi.org/10.1111/j.1525-1594.2010.01106.x
- [53] T.J. Gundert, A.L. Marsden, W. Yang, J.F. Ladisa, Optimization of cardiovascular stent design using computational fluid dynamics. J. Biomech. Eng. 134 (1), 1-8 (2012). DOI: https://doi.org/10.1115/1.4005542
- [54] S. Pant, N.W. Bressloff, A.I.J. Forrester, N. Curzen, The influence of strut-connectors in stented vessels: A comparison of pulsatile flow through five coronary stents. Ann. Biomed. Eng. 38, 1893-1907 (2010).
  DOI: https://doi.org/10.1007/s10439-010-9962-0
- [55] L. Jing, T.J. Webster, Endothelial cell adhesion on highly controllable compared to random nanostructured titanium surface features. Mater. Res. Soc. Symp. Proc. 951, 287-293 (2006). DOI: https://doi.org/10.1557/proc-0951-e12-29
- [56] K. Yuan, C. Deng, L. Tan, X. Wang, W. Yan, X. Dai, et al., Structural and temporal dynamics analysis of zinc-based biomaterials: History, research hotspots and emerging trends. Bioact. Mater. 35, 306-329 (2024).
  DOI: https://doi.org/10.1016/j.bioactmat.2024.01.017
- [57] Y. Su, H. Yang, J. Gao, Y. X. Qin, et al., Interfacial zinc phosphate is the key to controlling biocompatibility of metallinc zinc implants. Adv. Scie. 6, 1900112 (2019). DOI: https://doi:10.1002/advs.201900112
- [58] Y. Wen, Y. Li, R. Yang, Y. Chen, Y. Shen, Y. Liu, et al., Biofunctional coatings and drug-coated stents for restenosis therapy. Mater. Today. Bio. 29, 101259 (2024).
  DOI: https://doi.org/10.1016/j.mtbio.2024.101259
- [59] S. McMahon, N. Bertollo, E.D. O'Cearbhaill, J. Salber, L. Pierucci, P. Duffy, et al., Bio-resorbable polymer stents: a review of material progress and prospects. Prog. Polym. Sci. 83, 79-96 (2018). DOI: https://doi.org/10.1016/j.progpolymsci.2018.05.002
- [60] S.N. Sehgal, Sirolimus: Its discovery, biological properties, and mechanism of action. Transplant. Proc. 35 (3), S7-S14 (2003). DOI: https://doi.org/10.1016/S0041-1345(03)00211-2
- [61] K. McKeage, D. Murdoch, K.L. Goa, The sirolimus-eluting stent: A review of its use in the treatment of coronary artery disease. Am. J. Cardiovasc. Drugs. 3, 211-230 (2003). DOI: https://doi.org/10.2165/00129784-200303030-00007

- [62] J.M. Seitz, K. Collier, E. Wulf, D. Bormann, N. Angrisani, A. Meyer-Lindenberg, et al., The effect of different sterilization methods on the mechanical strength of magnesium based implant materials. Adv. Eng. Mater. 13 (12), 1146-1151 (2011). DOI: https://doi.org/10.1002/adem.201100074
- [63] P. Li, W. Zhang, S. Spintzyk, E. Schweizer, S. Krajewski, D. Alexander, et al., Impact of sterilization treatments on biodegradability and cytocompatibility of zinc-based implant materials. Mater. Sci. Eng. C. 130, 112430 (2021).
  DOI: https://doi.org/10.1016/j.msec.2021.112430
- [64] Z.Z. Shi, X.X. Gao, H.J. Zhang, X.F. Liu, H.Y. Li, C. Zhou, et al., Design biodegradable Zn alloys: Second phases and their significant influences on alloy properties. Bioact. Mater. 5 (2), 210-218 (2020). DOI: https://doi.org/10.1016/j.bioactmat.2020.02.010
- [65] K. Malisz, B. Świeczko-Żurek, Vascular stents materials and manufacturing technologies. Eng. Biomater. 166, 22-28 (2022). DOI: https://doi.org/10.34821/eng.biomat.166.2022.22-28
- [66] A.J. Drelich, S. Zhao, R.J. Guillory, J.W. Drelich, J. Goldman, Long-term surveillance of zinc implant in murine artery: Surprisingly steady biocorrosion rate. Acta. Biomater. 58, 539-549 (2017). DOI: https://doi.org/10.1016/j.actbio.2017.05.045
- [67] S. Zhao, J.M. Seitz, R. Eifler, H.J. Maier, R.J. Guillory, E.J. Earley, et al., Zn-Li alloy after extrusion and drawing: Structural, mechanical characterization, and biodegradation in abdominal aorta of rat. Mater. Sci. Eng. C. 76, 301-312 (2017).
  DOI: https://doi.org/10.1016/j.msec.2017.02.167
- [68] H. Jin, S. Zhao, R. Guillory, P.K. Bowen, Z. Yin, A. Griebel, et al., Novel high-strength, low-alloys Zn-Mg (< 0.1 wt% Mg) and their arterial biodegradation. Mater. Sci. Eng. C. 84, 67-79 (2018). DOI: https://doi.org/10.1016/j.msec.2017.11.021</p>
- [69] R.J. Guillory, M. Sikora-Jasinska, J.W. Drelich, J. Goldman, In Vitro Corrosion and in Vivo Response to Zinc Implants with Electropolished and Anodized Surfaces. ACS. Appl. Mater. Inter. 11, 19884-19893 (2019). DOI: https://doi.org/10.1021/acsami.9b05370
- [70] C. Hartl, Review on advances in metal micro-tube forming. Metals. **9** (5), 542 (2019). DOI: https://doi.org/10.3390/met9050542
- [71] X. Liu, J. Sun, Y. Yang, Z. Pu, Y. Zheng, In vitro investigation of ultra-pure Zn and its mini-tube as potential bioabsorbable stent material. Mater. Lett. 161, 53-56 (2015). DOI: https://doi.org/10.1016/j.matlet.2015.06.107
- [72] C. Wang, Z. Yu, Y. Cui, Y. Zhang, S. Yu, G. Qu, et al., Processing of a Novel Zn Alloy Micro-Tube for Biodegradable Vascular Stent Application. J. Mater. Sci. Technol. 32 (9), 925-929 (2016). DOI: https://doi.org/10.1016/j.jmst.2016.08.008
- [73] Y. Dai, Y. Zhang, H. Liu, H. Fang, D. Li, X. Xu, et al., Mechanical strengthening mechanism of Zn-Li alloy and its mini tube as potential absorbable stent material. Mater. Lett. 235, 220-223 (2019). DOI: https://doi.org/10.1016/j.matlet.2018.10.001
- [74] Y. Ren, D. Lou, M. Zhang, M. Lv, H. Li, G. Qin, Fabrication, Microstructures, and Mechanical Properties of Zn-0.1Mg-1Mn (wt.%) Alloy Tube. J. Mater. Eng. Perform. 32, 793-802 (2023). DOI: https://doi.org/10.1007/s11665-022-07122-7
- [75] D. Lou, M. Zhang, Y. Ren, H. Li, G. Qin, Fabrication of Zn-0.5Mn-0.05 Mg Micro-Tube with Suitable Strength and Ductility

- for Vascular Stent Application. Acta. Metall. Sin-Engl. **38**, 327-337 (2025). DOI: https://doi.org/10.1007/s40195-024-01782-1
- [76] V. Senthilkumar, Laser cutting process A Review. Int. J. Darshan. Inst. Eng. Res. Emerg. Technol. 3 (1), 44-48 (2014). Available on website: https://shorturl.at/08JIz
- [77] A.J. Guerra, J. Ciurana, Stent's Manufacturing Field: Past, Present, and Future Prospects, in: B. Pamukçu (Eds.), Angiography, IntechOpen (2019). DOI: https://doi.org/10.5772/intechopen.81668
- [78] H. Yang, C. Wang, C. Liu, H. Chen, Y. Wu, J. Han, et al., Evolution of the degradation mechanism of pure zinc stent in the one-year study of rabbit abdominal aorta model. Biomaterials. 145, 92-105 (2017). DOI: https://doi.org/10.1016/j.biomaterials.2017.08.022
- [79] G. Catalano, A.G. Demir, V. Furlan, B. Previtali. Erratum: Prototyping of biodegradable flat stents in pure zinc by laser microcutting and chemical etching. J. Micromech. Microeng. 28, 109601 (2018). DOI: https://doi.org/10.1088/1361-6439/aacfbb
- [80] C. Zhou, H.F. Li, Y.X. Yin, Z.Z. Shi, T. Li, X.Y. Feng, et al., Long-term in vivo study of biodegradable Zn-Cu stent: A 2-year implantation evaluation in porcine coronary artery. Acta. Biomater. 97, 657-670 (2019). DOI: https://doi.org/10.1016/j.actbio.2019.08.012
- [81] S. Lin, X. Ran, X. Yan, W. Yan, Q. Wang, T. Yin, et al., Corrosion behavior and biocompatibility evaluation of a novel zinc-based alloy stent in rabbit carotid artery model. J. Biomed. Mater. Res. - Part. B. Appl. Biomater. 107 (6), 1814-1823 (2019). DOI: https://doi.org/10.1002/jbm.b.34274
- [82] C. Zhou, X. Feng, Z. Shi, C. Song, X. Cui, J. Zhang, et al., Research on elastic recoil and restoration of vessel pulsatility of Zn-Cu biodegradable coronary stents. Biomed. Tech. 65 (2), 219-227 (2019). DOI: https://doi.org/10.1515/bmt-2019-0025
- [83] J. Jiang, H. Huang, J. Niu, D. Zhu, G. Yuan, Fabrication and characterization of biodegradable Zn-Cu-Mn alloy micro-tubes and vascular stents: Microstructure, texture, mechanical properties and corrosion behavior. Acta. Biomater. 151, 647-660 (2022). DOI: https://doi.org/10.1016/j.actbio.2022.07.049
- [84] Y. Qian, Y. Chen, J. Jiang, J. Pei, J. Li, J. Niu, et al., Biosafety and efficacy evaluation of a biodegradable Zn-Cu-Mn stent: A long-term study in porcine coronary artery. Bioact .Mater. **45**, 231–245 (2025). DOI: https://doi.org/10.1016/j.bioactmat.2024.11.022
- [85] X. Zhang, J. Niu, K.W.K. Yeung, H. Huang, Z. Gao, C. Chen, et al., Developing Zn-2Cu-xLi (x < 0.1 wt %) alloys with suitable mechanical properties, degradation behaviors and cytocompatibility for vascular stents. Acta. Biomater. (2024). DOI: https://doi.org/10.1016/j.actbio.2024.06.007
- [86] B.S.P.K. Kandala, G. Zhang, C. LCorriveau, M. Paquin, M. Chagnon, D. Begun, et al., Preliminary study on modelling, fabrication by photo-chemical etching and in vivo testing of biodegradable magnesium AZ31 stents. Bioact. Mater. 6 (6), 1663–1675 (2021). DOI: https://doi.org/10.1016/j.bioactmat.2020.11.012
- [87] B.S.P.K. Kandala, G. Zhang, T.M. Hopkins, X. An, S.K. Pixley, V. Shanov, In vitro and in vivo testing of zinc as a biodegradable material for stents fabricated by photo-chemical etching. Appl. Sci. 9 (21), 4503 (2019). DOI: https://doi.org/10.3390/app9214503
- [88] S. Chen, T. Du, H. Zhang, J. Qi, Y. Zhang, Y. Mu, et al., Methods for improving the properties of zinc for the application of bio-

- degradable vascular stents. Biomater. Adv. **156**, 213693 (2024). DOI: https://doi.org/10.1016/j.bioadv.2023.213693
- [89] Y. Qin, P. Wen, H. Guo, D. Xia, Y. Zheng, L. Jauer, et al., Additive manufacturing of biodegradable metals: Current research status and future perspectives. Acta. Biomater. 98, 3–22 (2019). DOI: https://doi.org/10.1016/j.actbio.2019.04.046
- [90] P. Wen, Y. Qin, Y. Chen, M. Voshage, L. Jauer, R. Poprawe, et al., Laser additive manufacturing of Zn porous scaffolds: Shielding gas flow, surface quality and densification. J. Mater. Sci. Technol. 35 (2), 368–376 (2019). DOI: https://doi.org/10.1016/j.jmst.2018.09.065
- [91] M. Montani, A.G. Demir, E. Mostaed, M. Vedani, B. Previtali, Processability of pure Zn and pure Fe by SLM for biodegradable metallic implant manufacturing. Rapid. Prototyp. J. 23 (3), 514–523 (2017). DOI: https://doi.org/10.1108/RPJ-08-2015-0100
- [92] P. Wen, L. Jauer, M. Voshage, Y. Chen, R. Poprawe, J.H. Schleifenbaum, Densification behavior of pure Zn metal parts produced by selective laser melting for manufacturing biodegradable implants. J. Mater. Process. Technol. 258, 128–137 (2018). DOI: https://doi. org/10.1016/j.jmatprotec.2018.03.007
- [93] P. Wen, M. Voshage, L. Jauer, Y. Chen, Y. Qin, R. Poprawe, et al., Laser additive manufacturing of Zn metal parts for biodegradable applications: Processing, formation quality and mechanical properties. Mater. Des. 155, 36–45 (2018). DOI: https://doi. org/10.1016/j.matdes.2018.05.057
- [94] M. Voshage, S. Megahed, P.G. Schückler, P. Wen, Y. Qin, L. Jauer, et al., Additive manufacturing of biodegradable Zn-xMg alloys: Effect of Mg content on manufacturability, microstructure and mechanical properties. Mater. Today. Commun. 32, 103805 (2022). DOI: https://doi.org/10.1016/j.mtcomm.2022.103805
- [95] J. Ning, Z.X. Ma, L.J. Zhang, D.P. Wang, S.J. Na, Effects of magnesium on microstructure, properties and degradation behaviors of zinc-based alloys prepared by selective laser melting. Mater. Res. Express. 9 (8), 086511 (2022).
  DOI: https://doi.org/10.1088/2053-1591/ac88b7
- [96] Y. Qin, P. Wen, D. Xia, H. Guo, M. Voshage, L. Jauer, et al., Effect of grain structure on the mechanical properties and in vitro corrosion behavior of additively manufactured pure Zn. Addit. Manuf. 33, 101134 (2020).
  - DOI: https://doi.org/10.1016/j.addma.2020.101134

- [97] C. Wang, Y. Hu, C. Zhong, C. Lan, W. Li, X. Wang, Microstructural evolution and mechanical properties of pure Zn fabricated by selective laser melting. Mater. Sci. Eng. A. 846, 143276 (2022). DOI: https://doi.org/10.1016/j.msea.2022.143276
- [98] Y. Qin, J. Liu, Y. Chen, P. Wen, Y. Zheng, Y. Tian, et al., Influence of laser energy input and shielding gas flow on evaporation fume during laser powder bed fusion of Zn metal. Materials. 14 (10), 2677 (2021). DOI: https://doi.org/10.3390/ma14102677
- [99] M. Yang, L. Yang, S. Peng, F. Deng, Y. Li, Y. Yang, et al., Laser additive manufacturing of zinc: formation quality, texture, and cell behavior. Bio-Des. Manuf. 6, 103-120 (2023). DOI: https://doi.org/10.1007/s42242-022-00216-0
- [100] Z. Dong, C. Han, G. Liu, J. Zhang, Q. Li, Y. Zhao, et al., Revealing anisotropic mechanisms in mechanical and degradation properties of zinc fabricated by laser powder bed fusion additive manufacturing. J. Mater. Sci. Technol. 214, 87-104 (2025). DOI: https://doi.org/10.1016/j.jmst.2024.06.045
- [101]M. Waqas, D. He, Z. Tan, P. Yang, M. Gao, X. Guo, A study of selective laser melting process for pure zinc and Zn10mg alloy on process parameters and mechanical properties. Rapid. Prototyp. J. 29 (9), 1923-1939 (2023). DOI: https://doi.org/10.1108/RPJ-04-2022-0138
- [102]K. Li, Y. Zhai, J. Zhu, X. Hu, C. Su, Y. Kong, et al., Effect of building orientation on the in vitro corrosion of biomedical Zn-Cu alloys prepared by selective laser melting. Corros. Sci. 231, 111957 (2024).
  - DOI: https://doi.org/10.1016/j.corsci.2024.111957
- [103] A. Liu, Y. Qin, J. Dai, F. Song, Y. Tian, Y. Zheng, et al., Fabrication and performance of Zinc-based biodegradable metals: From conventional processes to laser powder bed fusion. Bioact. Mater. 41, 312-335 (2024).
  - DOI: https://doi.org/10.1016/j.bioactmat.2024.07.022
- [104] C. Chen, R. Yue, J. Zhang, et al., Biodegradable Zn-1.5Cu-1.5Ag alloy with anti-aging ability and strain hardening behavior for cardiovascular stents. Mater. Sci. Eng. C. 116, 111172 (2020). DOI: https://doi.org/10.1016/j.msec.2020.111172
- [105]C. Chen, J. Chen, W. Wu, et al., In vivo and in vitro evaluation of a biodegradable magnesium vascular stent designed by shape optimization strategy. Biomaterials **221**, 119414 (2019). DOI: https://doi.org/10.1016/j.biomaterials.2019.119414